

Elastic Lattices Inspired by Ulam-Warburton Cellular Automaton

Hasan B. Al Ba'ba'a

Department of Mechanical Engineering, Union College, Schenectady, NY 12308, USA

albabaah@union.edu

Periodic lattices have been predominantly explored for decades, owing to their peculiar vibrational behavior. On the other hand, certain types of aperiodic lattices have enabled new phenomena that may not be otherwise attainable in periodic ones. In this paper, a new class of aperiodic lattices inspired by cellular automaton is introduced. Cellular automaton was originally developed as a machine replication algorithm and it has been intensively explored in computer science. These algorithms yield structures that are not necessarily periodic, yet follow well-defined rules that lead to interesting aperiodic patterns. The concept is utilized here to build elastic lattices following such rules, and Ulam-Warburton Cellular Automaton (UWCA) is demonstrated as an example. Resulted UWCA lattices are shown to exhibit unique dynamical properties, including symmetric eigenfrequency spectra, repeated natural frequencies of large multiplicity, and the emergence of strongly localized corner modes. It is envisioned that computer-algorithm-inspired lattices may unlock new wave phenomena that could outperform existing lattice designs.

Keywords

Cellular automaton, Ulam-Warburton, natural frequencies, mode multiplicity, corner modes, fractal structures.

Engineered structural materials, often referred to as Phononic Materials (PMs), have revolutionized the design of vibratory structures. The word “phononic” has become customarily associated with periodicity in structural design, i.e., structures built from a self-repeating block called unit cells [1]. In contrast to naturally occurring materials and composites, PMs exhibit an exceptional ability to enable a plethora of intriguing and unconventional phenomena in both acoustic and elastic media [1, 2]. Among the prime examples are frequency bandgaps [3–6] (i.e., frequency ranges of blocked wave propagation), single or double negative materials [7, 8], and high refractive index [9, 10]. As such, several potential applications of such PM systems have recently emerged. Examples include, but are not limited to, noise control and low-transmission of sound [11–13], flow stabilization [14, 15], acoustic logic gates [16], energy harvesting [17], cloaking [18, 19], topologically protected wave guiding [20–22], non-reciprocal wave transmission [23–25], among others [26, 27].

In elastic systems, a particularly interesting class of PMs is lattices, which are defined as structures built from simple interconnected elastic elements like rod, beams, and plates. Being relatively lightweight and exhibiting unique mechanical properties, lattices have enabled a variety of phenomena in wave propagation domain, such as wave directionality [28], energy harvesting [29], cloaking [30], and zero-energy modes [31, 32]. In the lattice design front, optimization techniques have been applied, for instance, to allow for better bandgap engineering [33, 34] and topological protection [35]. More related to this study is fractal-inspired designs of lattices’ unit cell. As a case in point, lattices with Koch fractal design have demonstrated some level of control over bandgaps by using

different number of iterations of the fractal, such that the frequency at which the first bandgap opens decreases as the fractal iteration number increases [36]. Another study has shown direct influence of fractal design on altering the elastic constant tensor, which in turn leads to different elastic response and generated bandgaps, where the latter is greatly affected by the fractal-cut symmetry of the unit cell [37]. Fibonacci-based structures have also been studied, yielding interesting patterns in their eigenfrequencies/bandgaps, which have been correlated with the Fibonacci sequence [38, 39]. Finally, bioinspired designs (comprising nacre, spider-webs, chohlea, moth-wings, and fractal structural shapes) have recently garnered research interest, and numerous studies in this domain have been encapsulated in a review by Dal Poggetto [40].

Beyond advancements in structural design, the embodiment of smart materials in lattices has proven useful in enabling exceptional features, including (i) self-healing to improve their life span [41], (ii) magnetoactive capabilities to control lattice spacing via remotely applied magnetic fields [42, 43], (iii) remarkable stretchability by means of elastomers [44, 45], (iv) thermal tunability of bandgaps by leveraging temperature dependence of elastic moduli [46], and (v) concurrent vibration suppression and energy harvesting via piezoelectric ceramics [47].

While periodic lattices have been a focal point of research for a few decades, the notion of aperiodicity and exploring new ways for manipulating and controlling waves is becoming rather appealing. As a case in point, quasi-periodicity has been shown to enable topologically protected edge states with various edge modes’ localization [48, 49]. Additionally, the concept of topological pumping, where a two-dimensional structure is adiabatically

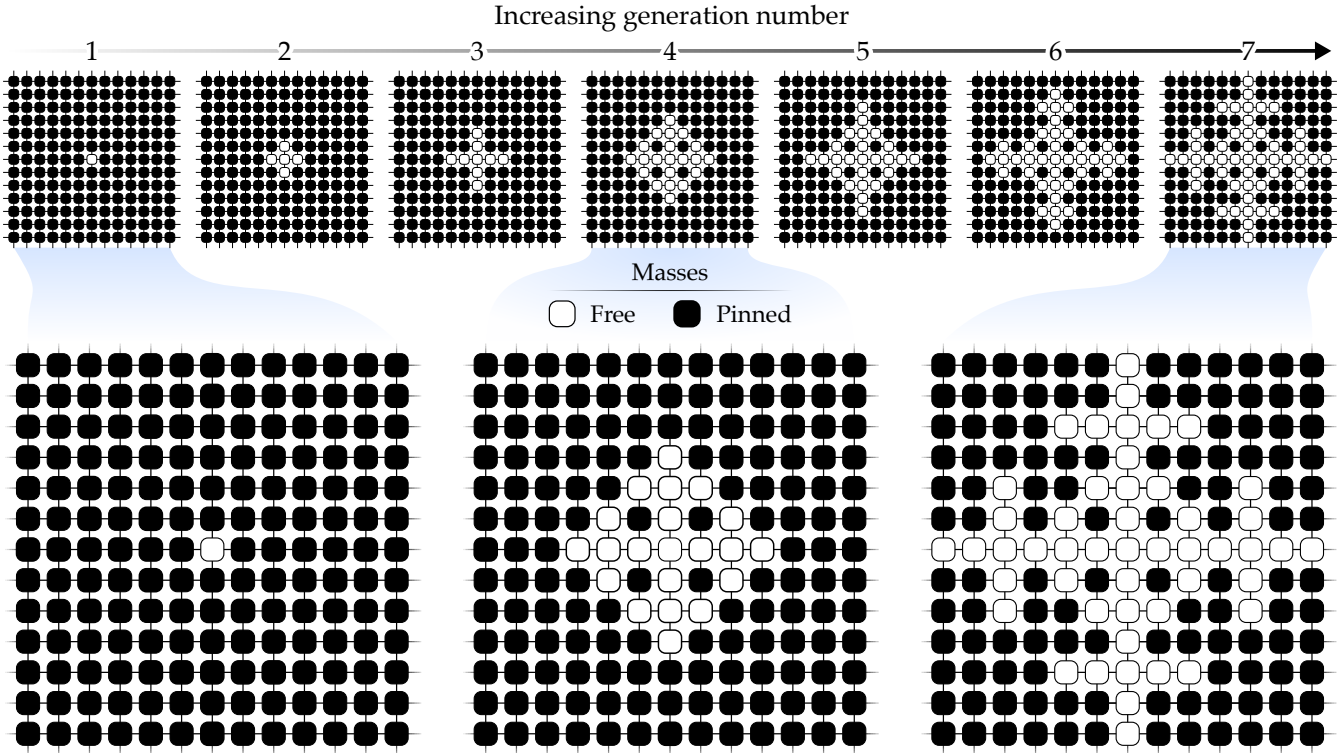


Figure 1: Elastic square lattice inspired by Ulam-Warbutron Cellular Automaton (UWCA), showing the first seven generations. The initial (zeroth) generation starts as a two-dimensional infinite monatomic lattice with pinned (or “OFF”) masses m , interconnected via springs of stiffness k . The first generation is enabled by turning the central mass “ON”, which is interpreted here as unpinning the central mass so it is free to move. Subsequent generations are determined by unpinning the masses that share a spring connection with exactly one unpinned (or an “ON”) mass, as dictated by the UWCA algorithm. Close-ups of the first, fourth, and seventh generations are provided for reference.

modulated to gradually pump a signal from one corner to an opposite one, has been experimentally and theoretically achieved [50, 51]. Quasi-periodicity has also enabled the concept of near zero modes called floppy modes, which are a class of topological modes in Maxwell lattices [52]. Analogously, the concept of rainbow trapping, achieved by an array of resonators with a change in the system parameters that are not necessarily periodic (e.g., Ref. [53]), has been used for vibration isolation [54], and energy harvesting [55]. Owing to the promise of lattices that are unique in design and not necessarily periodic, and the need for novel approaches to control elastic/acoustic waves, I take inspiration from Cellular Automaton (CA) to introduce a new class of lattice designs. By definition, CA is a discrete computation model that has been used in computer science for many applications, thanks to its inventor von Neumann who developed it in the 1950s [56]. Since its inception, CA has been adopted by many fields of study. For instance, a biological object can be considered a quantifiable entity by numbers, and these numbers can relay how the different objects can self-replicate and influence each other. Having CA as a universal computational methodology for machine self-replication [57, 58], such algorithms are utilized to computationally model

and understand such biological entities and living organisms, such as protein, RNA, and DNA [59]. In physics, CA has been influential in studying many systems, including (i) the behavior of sand piles subject to a blow of wind [60], (ii) computational development of traffic flow problems [61], and (iii) statistical mechanics [62]. More pertinent studies to this work are (i) the use of hybrid CA, a computational method originally developed to understand the structural bones adaptation [63], to optimally design piezoelectric patches anchored to vibrational skin for maximizing its power output [64], and (ii) the characterization of fracture behavior in elastic bodies under dynamical loading via continuous-discontinuous CA [65].

For the sake of illustration, I demonstrate here a lattice design based on Ulam-Warbutron cellular automaton (UWCA), named after the contributions of Ulam and Warbutron [66], not to mention its popularity in mathematical circles [66–68]. The UWCA algorithm can be explained via an infinite sheet of packed square cells. These square cells can be in a state of “ON” or “OFF” (may also be interpreted as “1” or “0” or “dead” or “alive” cells). Initially, a pristine set of squares is set at an “OFF” state, and one single square is turned “ON” in its center. The rule for UWCA mandates that the neighboring “OFF” squares

turn “ON” *only* if they have a single edge shared with an “ON” square. If an “OFF” square cell shares two or more edges with “ON” cells, that square does not get activated (i.e., turned “ON”). Every stage the pattern grows is called a generation [67] (shall be assigned the variable n_g henceforth), and researchers have studied these patterns to predict the growth after a known number of generations [68]. An additional rule for the considered Ulam-Warburton CA is that if an “OFF” cell becomes “ON” at any given generation, it stays “ON” throughout future generations. Note that UWCA rules can be applied to other regular shapes, like a hexagon or triangle [67].

To demonstrate UWCA in elastic lattices, an elastic square monatomic lattice, constituting identical masses m that are interconnected via identical springs k and exhibit out-of-plane motion, is considered [1]. Implementing the rules of UWCA requires defining “OFF” and “ON” states in the context of a vibratory square lattice. To this end, the “OFF” state is interpreted as a “pinned” mass, i.e., a mass that is constrained from motion, and vice versa for the “ON” state. Following UWCA rules, a monatomic lattice with all masses at the “OFF” state (i.e., pinned) is the starting point, and the mass at the lattice’s center is then turned “ON” (i.e., unpinned). Moving forward with an increasing number of UWCA generations, interesting patterns grow, having more degrees of freedom after each generation due to the increasing number of unpinned masses. Schematics of the first seven generations of the UWCA lattice are depicted in Figure 1.

To understand the UWCA lattice dynamics, the natural modes are computed at different numbers of generations. To do so, I start by stating the equations of motion for the UWCA lattice. After assembling the stiffness and mass matrices at a given generation, and denoting n as the lattice’s degrees of freedom, the equations of motion can be written in the matrix form as:

$$\mathbf{M}\ddot{\mathbf{u}} + \mathbf{K}\mathbf{u} = \mathbf{f} \quad (1)$$

where \mathbf{M} and \mathbf{K} are the mass and stiffness matrices, respectively, while

$$\mathbf{u} = \{u_1 \quad u_2 \quad \dots \quad u_n\}^T \quad (2a)$$

$$\mathbf{f} = \{f_1 \quad f_2 \quad \dots \quad f_n\}^T \quad (2b)$$

are the displacement and the forcing vectors, respectively. The degrees of freedom are numbered starting from left to right in the bottom row of the lattice and the process is repeated row by row until its top row. Given the discrete nature of the lattices, and uniform values of masses, the mass matrix is a constant diagonal matrix $\mathbf{M} = m\mathbf{I}$, where \mathbf{I} is an identity matrix of size $n \times n$. The stiffness matrix \mathbf{K} is assembled based on the connectivity of the masses, which is different for various generations of UWCA (Examples of the stiffness matrix are provided in the supplementary materials). A common characteristic of \mathbf{K} in all

generations of UWCA lattice is the constant diagonal elements of $4k$, which will facilitate the discussion on its eigenvalues shortly. Introducing $\mathbf{M}^{-1}\mathbf{K} = \omega_0^2\mathbf{D}$, where $\omega_0 = \sqrt{k/m}$, and applying the harmonic solution in the absence of forces, Equation (1) reduces to $\mathbf{D}\mathbf{u} = \lambda\mathbf{u}$, i.e., an eigenvalue problem with eigenvalues $\lambda = \omega^2/\omega_0^2$ and ω being the frequency.

Solving the eigenvalue problem using MATLAB, the eigenvalues (and thus the natural frequencies) are calculated for different generations n_g , as shown in Figure 2(a) for the first eleven generations. As seen in the figure, the results are depicted as a three-dimensional plot, where the axes denote the natural frequency (normalized in units of ω_0), the number of degrees of freedom (n) in a logarithmic scale of base 10, and, the number of generation (n_g), respectively. It is observed that the natural frequencies are bounded between $\omega/\omega_0 \approx 1.2$ and $\omega/\omega_0 \approx 2.6$, owing to the discrete nature of the lattice. While an upper cutoff frequency is a known characteristic of discrete lattices, the lower cutoff frequency in the UWCA lattice appears to be a byproduct of pinning, thus resembling a lattice with an elastic foundation [22, 69, 70]. Peculiarly, a signature of UWCA lattice dynamics is the repeated natural frequencies (the flat points in the figure), emerging at various frequencies (particularly at $\omega/\omega_0 = 2$), and their multiplicity depends on the overall shape of the structure at a given generation.

If the eigenvalues λ are plotted instead of the natural frequencies ω , interesting patterns are noted, as in Figure 2(b). It is noticed that all eigenvalues are distributed symmetrically about $\lambda = 4$. This becomes rather clear when the eigenvalues are shifted down by 4, given that \mathbf{D} has constant diagonal elements of the same magnitude, stemming from the constant diagonal elements of \mathbf{K} . This process results in a spectrum where every eigenvalue λ has a negative counterpart $-\lambda$, and being symmetric about zero instead of 4. Such symmetry in eigenvalues is akin to particle-hole symmetry in condensed matter systems [71]. Finally, the degrees of freedom n versus the number of generation n_g is depicted in Figure 2(c), showing a substantial increase in the degrees of freedom n as UWCA pattern grows with higher generations n_g .

Interestingly, some of the repeated natural frequencies observed in Figures 2(a,b) correspond to strong localization at the lattice’s corners, known as corner modes, which have witnessed a spurt in research interest recently [72–76]. These strongly-localized corner modes in UWCA lattices emerge at $\omega/\omega_0 = \sqrt{3}$ and $\omega/\omega_0 = \sqrt{5}$ (or $\lambda = 3$ and $\lambda = 5$) and only materialize when the generation number is according to this formula:

$$n_g = 4r - 1 \quad (3)$$

where r is an integer equal or larger than 2. As such, the number of generations n_g having these special corner modes must be odd numbers that start with seven at $r = 2$ and increase by four hereafter. At such generations, the

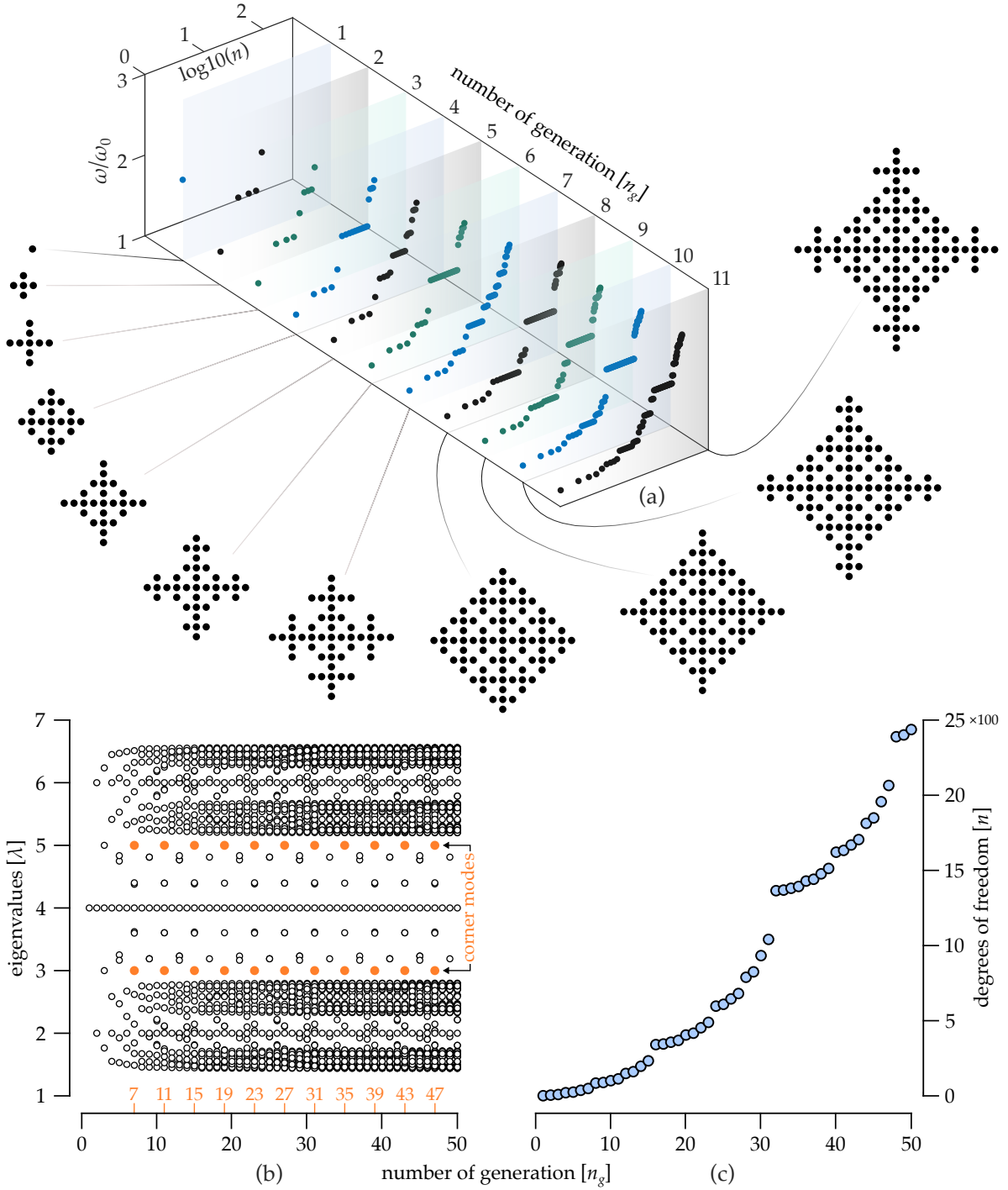


Figure 2: (a) The natural frequency spectra of elastic lattices built following the first eleven generations of UWCA. A schematic of the free (or “ON”) masses for each generation is depicted for reference. (b) The eigenvalue spectra of the UWCA lattice for an increasing number of generations, showing symmetry about $\lambda = 4$. Among those eigenvalues, there are corner modes (marked in orange for reference), which occur at odd numbers of generations, starting at seven and increasing by increments of four. (c) The degrees of freedom n versus the number of generation n_g is shown, demonstrating a considerable increase in the degrees of freedom n as UWCA pattern grows with higher generations n_g .

UWCA lattice has corners with a perpendicular-sign (\perp) shape, such that six masses stem equally in three directions. Each physical corner of the described shape corre-

sponds to two repeated natural modes per frequency (i.e., two modes for each $\omega/\omega_0 = \sqrt{3}$ and $\omega/\omega_0 = \sqrt{5}$).

In Figure 3, the response of UWCA lattice near $\omega/\omega_0 =$

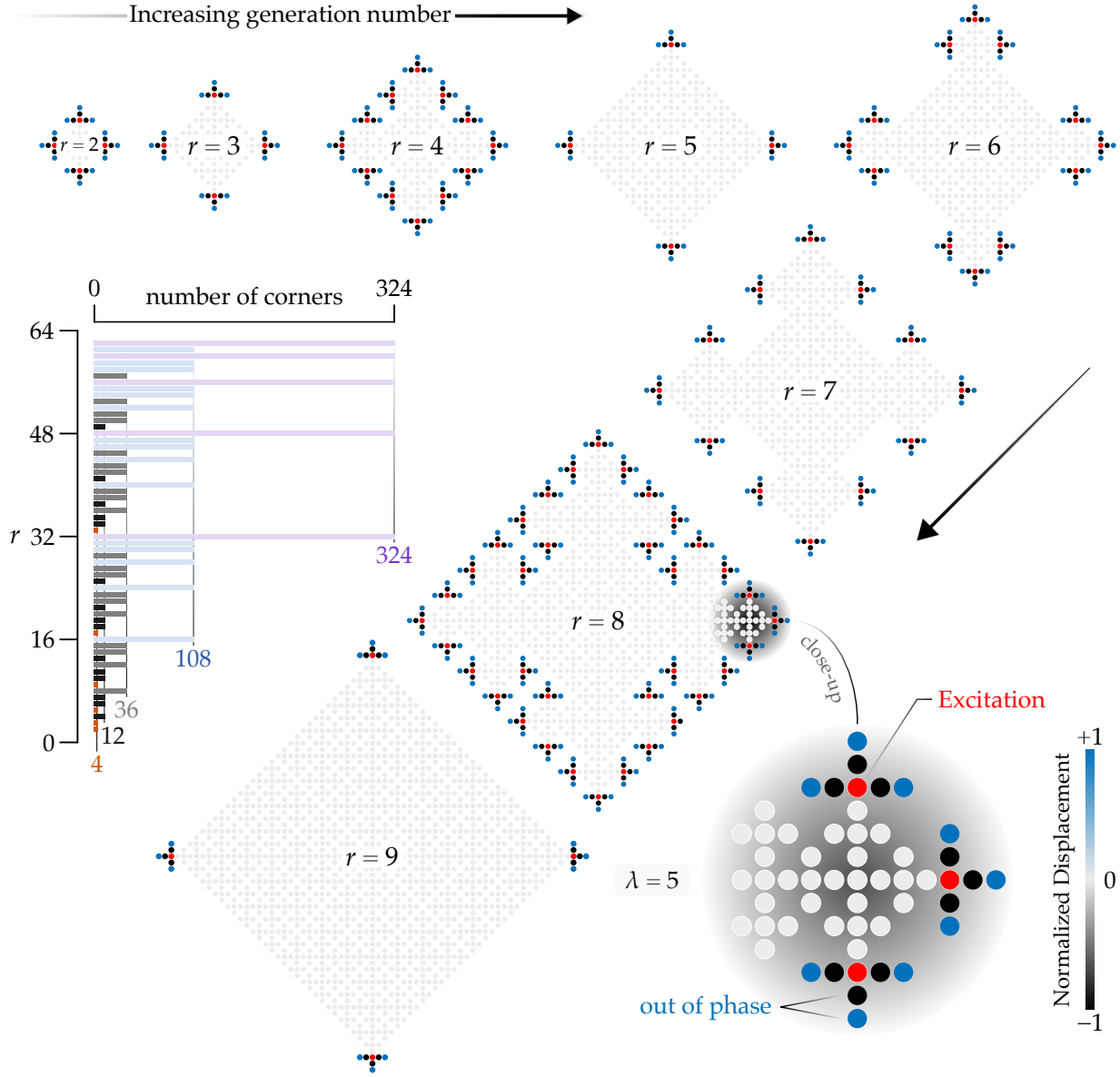


Figure 3: The normalized displacement response of UWCA lattice at the first eight generations with corners of \perp shape. Corner modes are excited at a frequency near $\omega = \sqrt{5}\omega_0$ (or $\lambda = 5$) by applying a force at the junction connecting the \perp shaped corner with the bulk of the lattice, which are colored as red for ease of reference. The bar chart in the middle of the figure shows the number of corners of \perp shape versus the integer r . The number of corners differs with various values of r (and generation number $n_g = 4r - 1$), but they reset to 4 whenever $r = 2^z$, where z is an integer equal or larger than 1. At such values, the number of corners reaches a local maximum.

$\sqrt{5}$ (to avoid numerical singularity at $\sqrt{5}$) are shown for eight successive generations having corner modes ($r = 2$ through $r = 9$), where the displacement is normalized and its magnitude is reflected by the color legend. To excite the corner modes, forces are applied at the conjunction of the \perp shapes with the lattice's bulk, and are marked as red circles for ease of reference. As can be seen in the figure, the bulk is nearly motionless, while the corner masses respond to the excitations near $\omega/\omega_0 = \sqrt{5}$. Regardless of the value of integer r , the corner masses oscillate out of

phase, as illustrated in the close-up of one of the corners in $r = 8$ case. If the excitation is near $\omega/\omega_0 = \sqrt{3}$ instead, i.e., the other natural frequency that exhibits corner modes, then the corner masses shall move in phase.

It is crucial to shed light on the number of corners of \perp shape with different values of r . In the middle of Figure 3, the number of corners for a swept range of r is depicted, for which the following observations are drawn:

1. The number of corners does not necessarily increase with increasing r .

2. Whenever $r = 2^z + 1$, corresponding to $n_g = 2^{z+2}$, with z being an integer greater than 1, the number of corners resets to four. Observe, for instance, $r = 5$ and $r = 9$ cases (corresponding to $z = 1$ and $z = 2$, respectively), which are the successive integers of $r = 2^2 = 4$ and $r = 2^3 = 8$, respectively.
3. Following the previous point, the number of corners locally maximizes at $n_g = 2^{z+2} - 1$ right before it abruptly drops to 4 at the subsequent generation, i.e., $n_g = 2^{z+2}$.
4. It is worth mentioning that the local maximum number of corners seems to grow with increasing z (and, thus, increasing r) and each new maximum is triple the previous one as deduced from the sequence 4, 12, 36, 108, and 324 in the figure (corresponding to $r = 2^1, 2^2, 2^3, 2^4$, and 2^5 , respectively).

In summary, this paper introduced a new class of aperiodic lattices inspired by Ulam-Warburton Cellular Automaton (UWCA). The algorithm of UWCA starts with infinite packed squares that are initially “OFF”, and the squares are then turned “ON” following specific rules.

Such an algorithm results in aperiodic structures of an increasing number of “ON” squares that grow larger with higher numbers of generations. Identical procedure is applied here to an infinite elastic monatomic lattice by interpreting the “OFF” (“ON”) state as pinned (unpinned) mass. Lattices built through UWCA algorithm are demonstrated to exhibit unique dynamical properties (e.g., corner modes), as revealed by their eigenfrequency spectra.

Future directions of this research can include (1) exploring various types of CA algorithms for unique lattice designs and characteristics, (2) the study of damping characteristics to observe whether these lattice structures give rise to amplified damping (e.g., metadamping [77–80]), (3) investigating the effective elastic and inertial properties of these novel lattices, especially that lattices are known to be unique in that regard [81], (4) incorporating materials with tunable mechanical properties in their design (e.g., magnetoactive materials [42]), and (5) extending the same concept to acoustic lattices or LC-circuit networks. Work is in progress to explore similar classes of structures, called toothpick sequences [68], and determine their unique vibrational traits.

References

- [1] M. I. Hussein, M. J. Leamy, M. Ruzzene, *Applied Mechanics Reviews* **2014**, 66.
- [2] Y.-F. Wang, Y.-Z. Wang, B. Wu, W. Chen, Y.-S. Wang, *Applied Mechanics Reviews* **2020**, 72, 040801.
- [3] Z. Liu, X. Zhang, Y. Mao, Y. Zhu, Z. Yang, C. T. Chan, P. Sheng, *Science* **2000**, 289, 1734–1736.
- [4] H. Al Ba’ba’a, M. Nouh, T. Singh, *Journal of Sound and Vibration* **2017**, 410, 429–446.
- [5] M. I. Hussein, G. M. Hulbert, R. A. Scott, *Journal of sound and vibration* **2006**, 289, 779–806.
- [6] M. I. Hussein, G. M. Hulbert, R. A. Scott, *Journal of Sound and Vibration* **2007**, 307, 865–893.
- [7] V. M. García-Chocano, R. Graciá-Salgado, D. Torrent, F. Cervera, J. Sánchez-Dehesa, *Physical Review B* **2012**, 85, 184102.
- [8] R. Gracia-Salgado, D. Torrent, J. Sánchez-Dehesa, *New Journal of Physics* **2012**, 14, 103052.
- [9] Z. Liang, J. Li, *Physical review letters* **2012**, 108, 114301.
- [10] Y. Cheng, C. Zhou, B. Yuan, D. Wu, Q. Wei, X. Liu, *Nature materials* **2015**, 14, 1013.
- [11] Z. Yang, H. Dai, N. Chan, G. Ma, P. Sheng, *Applied Physics Letters* **2010**, 96, 041906.
- [12] N. Sui, X. Yan, T.-Y. Huang, J. Xu, F.-G. Yuan, Y. Jing, *Applied Physics Letters* **2015**, 106, 171905.
- [13] Y. Liao, H. Huang, G. Chang, D. Luo, C. Xu, Y. Wu, J. Tang, *Materials* **2022**, 15, 3261.
- [14] M. I. Hussein, S. Biringen, O. R. Bilal, A. Kucala, *Proceedings of the Royal Society A: Mathematical Physical and Engineering Sciences* **2015**, 471, 20140928.
- [15] A. Kianfar, M. I. Hussein, *New Journal of Physics* **2023**, 25, 053021.
- [16] J.-P. Xia, D. Jia, H.-X. Sun, S.-Q. Yuan, Y. Ge, Q.-R. Si, X.-J. Liu, *Advanced Materials* **2018**, 30, 1805002.
- [17] G. Hu, L. Tang, J. Liang, C. Lan, R. Das, *Smart Materials and Structures* **2021**.
- [18] L. Zigoneanu, B.-I. Popa, S. A. Cummer, *Nature materials* **2014**, 13, 352.
- [19] H. Nassar, Y. Chen, G. Huang, *Journal of the Mechanics and Physics of Solids* **2019**, 129, 229–243.
- [20] C. He, X. Ni, H. Ge, X.-C. Sun, Y.-B. Chen, M.-H. Lu, X.-P. Liu, Y.-F. Chen, *Nature Physics* **2016**, 12, 1124.
- [21] R. K. Pal, M. Ruzzene, *New Journal of Physics* **2017**, 19, 25001.
- [22] H. Al Ba’ba’a, X. Zhu, Q. Wang, *Proceedings of the Royal Society A* **2021**, 477, 20200820.
- [23] R. Fleury, D. L. Sounas, C. F. Sieck, M. R. Haberman, A. Alù, *Science* **2014**, 343, 516–519.
- [24] M. A. Attarzadeh, M. Nouh, *Journal of Sound and Vibration* **2018**, 422, 264–277.
- [25] M. Attarzadeh, J. Callanan, M. Nouh, *Physical Review Applied* **2020**, 13, 021001.
- [26] S. A. Cummer, J. Christensen, A. Alù, *Nature Reviews Materials* **2016**, 1, 16001.
- [27] S. Chen, Y. Fan, Q. Fu, H. Wu, Y. Jin, J. Zheng, F. Zhang, *Applied Sciences* **2018**, 8, 1480.
- [28] A. S. Phani, J. Woodhouse, N. Fleck, *The Journal of the Acoustical Society of America* **2006**, 119, 1995–2005.
- [29] S. Gonella, A. C. To, W. K. Liu, *Journal of the Mechanics and Physics of Solids* **2009**, 57, 621–633.
- [30] H. Nassar, Y. Chen, G. Huang, *Physical review letters* **2020**, 124, 084301.
- [31] T. Lubensky, C. Kane, X. Mao, A. Souslov, K. Sun, *Reports on Progress in Physics* **2015**, 78, 073901.
- [32] R. Xia, H. Nassar, H. Chen, Z. Li, G. Huang, *Journal of the Mechanics and Physics of Solids* **2021**, 155, 104564.
- [33] O. Sigmund, J. Søndergaard Jensen, *Philosophical Transactions of the Royal Society of London. Series A: Mathematical Physical and Engineering Sciences* **2003**, 361, 1001–1019.
- [34] O. R. Bilal, M. I. Hussein, *Physical Review E - Statistical Nonlinear and Soft Matter Physics* **2011**, 84, 65701.

- [35] Z. Du, H. Chen, G. Huang, *Journal of the Mechanics and Physics of Solids* **2020**, 135, 103784.
- [36] P. Zhao, K. Zhang, Z. Deng, *Acta Mechanica Solida Sinica* **2020**, 33, 600–611.
- [37] V. Kunin, S. Yang, Y. Cho, P. Deymier, D. J. Srolovitz, *Extreme Mechanics Letters* **2016**, 6, 103–114.
- [38] Z. Hou, F. Wu, Y. Liu, *Physica B: Condensed Matter* **2004**, 344, 391–397.
- [39] A. Bacigalupo, M. L. De Bellis, M. Vasta, *International Journal of Mechanical Sciences* **2022**, 224, 107280.
- [40] V. F. Dal Poggetto, *Frontiers in Materials* **2023**, 10, 1176457.
- [41] K. Yu, A. Xin, H. Du, Y. Li, Q. Wang, *NPG Asia Materials* **2019**, 11, 1–11.
- [42] K. Yu, N. X. Fang, G. Huang, Q. Wang, *Advanced Materials* **2018**, 30, 1706348.
- [43] K. H. Lee, H. Al Ba'ba'a, K. Yu, K. Li, Y. Zhang, H. Du, S. F. Masri, Q. Wang, *Advanced Science* **2022**, 9, 2201204.
- [44] Y. Jiang, Q. Wang, *Scientific reports* **2016**, 6, 1–11.
- [45] Y. Zhang, K. Yu, K. H. Lee, K. Li, H. Du, Q. Wang, *Journal of the Mechanics and Physics of Solids* **2022**, 159, 104782.
- [46] C. Nimmagadda, K. H. Matlack, *Journal of Sound and Vibration* **2019**, 439, 29–42.
- [47] Y. Li, E. Baker, T. Reissman, C. Sun, W. K. Liu, *Applied Physics Letters* **2017**, 111.
- [48] M. I. Rosa, Y. Guo, M. Ruzzene, *Applied Physics Letters* **2021**, 118, 131901.
- [49] M. Gupta, M. Ruzzene, *Crystals* **2020**, 10, 1144.
- [50] E. Riva, M. I. Rosa, M. Ruzzene, *Physical Review B* **2020**, 101, 094307.
- [51] M. I. Rosa, R. K. Pal, J. R. Arruda, M. Ruzzene, *Physical review letters* **2019**, 123, 034301.
- [52] D. Zhou, L. Zhang, X. Mao, *Physical Review X* **2019**, 9, 021054.
- [53] J. M. De Ponti, L. Iorio, E. Riva, R. Ardito, F. Braghin, A. Corigliano, *Physical Review Applied* **2021**, 16, 034028.
- [54] J. Zhang, X. Zhang, H. Zhang, X. Bi, N. Hu, C. Zhang, *Journal of Sound and Vibration* **2022**, 530, 116945.
- [55] B. Wang, Y. Huang, W. Zhou, Z. Yang, *Journal of Applied Physics* **2021**, 129, 064505.
- [56] X. Li, J. Wu, X. Li, et al., *Theory of practical cellular automaton*, Springer, **2018**.
- [57] P. Sarkar, *Acm computing surveys (csur)* **2000**, 32, 80–107.
- [58] J. Kari, *Theoretical computer science* **2005**, 334, 3–33.
- [59] P. P. Chaudhuri, S. Ghosh, A. Dutta, S. P. Choudhury, *A New Kind of Computational Biology: Cellular Automata Based Models for Genomics and Proteomics*, Springer, **2018**.
- [60] G. Cattaneo, M. Comito, D. Bianucci, *Theoretical Computer Science* **2012**, 436, 35–53.
- [61] S. Maerivoet, B. De Moor, *Physics reports* **2005**, 419, 1–64.
- [62] S. Wolfram, *Reviews of modern physics* **1983**, 55, 601.
- [63] A. TOVAR, N. M. PATEL, G. L. NIEBUR, M. SEN, J. E. RENAUD, *Journal of mechanical design* **2006**, 128, 1205–1216.
- [64] S. Lee, A. Tovar, *Journal of Mechanical Design* **2013**, 135, 031001.
- [65] F. Yan, P.-Z. Pan, X.-T. Feng, S.-J. Li, *Engineering Fracture Mechanics* **2018**, 204, 482–496.
- [66] M. Warburton, *arXiv preprint arXiv:1901.10565* **2019**.
- [67] S. Ulam et al. in Proceedings of symposia in applied mathematics, Vol. 14, American Mathematical Society Providence, RI, USA, **1962**, pp. 215–224.
- [68] D. Applegate, O. E. Pol, N. J. Sloane, *arXiv preprint arXiv:1004.3036* **2010**.
- [69] H. Al Ba'ba'a, M. Nouh, T. Singh, *The Journal of the Acoustical Society of America* **2017**, DOI 10.1121/1.5001513.
- [70] S. Nandi, T. Singh, M. Nouh, et al., *Journal of Applied Physics* **2020**, 127.
- [71] E. Prodan, K. Dobiszewski, A. Kanwal, J. Palmieri, C. Prodan, *Nature Communications* **2017**, 8, DOI 10.1038/ncomms14587.
- [72] M. Serra-Garcia, V. Peri, R. Süssstrunk, O. R. Bilal, T. Larsen, L. G. Villanueva, S. D. Huber, *Nature* **2018**, 555, 342–345.
- [73] H. Xue, Y. Yang, F. Gao, Y. Chong, B. Zhang, *Nature materials* **2019**, 18, 108–112.
- [74] H. Fan, B. Xia, L. Tong, S. Zheng, D. Yu, *Physical Review Letters* **2019**, 122, 204301.
- [75] H. Danawe, H. Li, H. A. Ba'ba'a, S. Tol, *Physical Review B* **2021**, 104, L241107.
- [76] H. B. Al Ba'ba'a, *Wave Motion* **2024**, 127, 103291.
- [77] M. I. Hussein, M. J. Frazier, *Journal of sound and vibration* **2013**, 332, 4767–4774.
- [78] D. DePauw, H. Al Ba'ba'a, M. Nouh, *Extreme Mechanics Letters* **2018**, 18, 36–44.
- [79] C. L. Bacquet, H. Al Ba'ba'a, M. J. Frazier, M. Nouh, M. I. Hussein, *Advances in Applied Mechanics* **2018**, 51, 115–164.
- [80] H. Al Ba'ba'a, Z. Lin, S. Tol, *Journal of Applied Physics* **2021**, 130, 184901.
- [81] S. Gonella, *Physical Review B* **2020**, 102, 140301.